Structural Health Monitoring and Intelligent Infrastructure, Wu & Abe (eds)
© 2003 Swets & Zeitlinger, Lisse, ISBN 90 5809 647 5

Measurement of stresses of large steel cables

M.L. Wang & G. Wang
Civil and Materials Engineering Department, the University of Illinois at Chicago, Chicago, Illinois, USA

ABSTRACT: In the construction of Qiangjiang No. 4 Bridge in Hangzhou, China, EM stress sensors are to be applied for accurate stress monitoring of the cable hangers. Based on the stress dependence of the magnetic properties of the steel, such as the relative permeability, the stress monitoring of the multi-strand cable via elastomagnetic (EM) stress sensor is discussed. Through series of tests undertaken on China 7 mm steel rod, experimental characterization concerning the tensile stress and temperature dependence of the relative permeability is generalized, and is applied to the stress monitoring of the multi-strand cable used in Qiangjiang No. 4 Bridge. Tests revealed that although mainly determined by the primary pulsed current, the magnetic field along the multi-strand cable is heavily affected by the location and the ferromagnetic surroundings of the EM stress sensors. For this reason, the working point (reflecting the primary current value where the permeability is measured) is regulated according to the magnetic field shift, therefore guarantees that the permeability is measured at the same field, regardless of the rearrangement of the ferromagnetic surroundings.

1 INTRODUCTION

The will-to-be constructed Qianjiang No. 4 Bridge in Hanzhou, China, is a double-layered bridge. The upper layer is designed for highway and the lower one is railway and pedestrian sidewalk. It is a concrete – steel tubes constituted hanger arc bridge. Each hanger is a HDPE covered structure, composed of dozens of single or twisted piano steel rods. The static stress analysis of the hangers plays a significant role in the health evaluation of the bridge. The elastomagnetic stress sensors presented below provides a reliable way of stress monitoring. Only the representative hangers most likely to be overstressed are considered, as indicated in Figure 1. Long since it has been discovered and extensively discussed that for most ferromagnetic materials the stress can change the magnetic properties (Joule 1842, Bozorth 1951, Cullity 1972, Mix 1987, Schneider et al. 1992, Stablik & Jiles 1993). This discovery began with the concept of magnetostriction, which indicates the magnetization of a magnetic material could reform its shape, as described below (Bozorth 1951):

$$\frac{1}{l}\frac{\partial l}{\partial H} = \frac{1}{4\pi}\frac{\partial B}{\partial \sigma} \qquad (1)$$

where l is length of the sample, H and B are respectively magnetic field and induction, σ is stress. It indicates that tension leads to the increase of induction, provided the material concerned being of positive magnetostriction. This phenomenon, as called magnetoelasticity, could also been inferred from the interaction of stress and magnetic domain orientations. Lots of researchers and engineers have explored its utilities in industry, especially in no-destructive examination (Mix 1987, Wang 1998, Wang 2001, Schaer 2002, 2003). As a promising application of magnetoelasticity in stress monitoring for cable-stayed or suspension bridges, etc., the elastomagnetic (EM) stress sensor discussed below is aimed to characterize the stress dependence of the magnetic properties, represented by the relative permeability.

The EM stress sensor is principally composed of primary coil and secondary coil (sensing coil), which work cooperatively to formalize the magnetoelastic characterization of the material. With pulsed current passing through the primary coil, the ferromagnetic material is being magnetized. As indicated in Figure 2, the pulse current in primary coil introduces as well a pulse magnetic field along the steel rod. The partial hysterisis curve (B-H curve) introduced is shown on the right. Initially a gentle upward trend is shown, then as H field reaches the maximal value and decreases, B field follows a gentle return too. The apparent relative permeability

$$\mu_r = \mu_0 \Delta B / \Delta H \qquad (2)$$

is measured in the descending section of the hysterisis curve, where ΔB and ΔH respectively signifies the variation in induction and magnetic field, and μ_0 is the permeability of the free space. However, to the EM stress sensor, the relative permeability is not derived directly from the hysterisis curve, or several uncertain variables would be unexpectedly introduced. In the present study is measured via the sensing coil following proper procedures (Wang 2001), as given below. The sensing coil picks up the induced electromotive force that is directly proportional to the change rate of the applied magnetic flux. During a small time interval $\Delta t1$, the flux variation through the secondary coil is:

$$\Delta\Phi_1=N[A_f(\Delta B)+(A_0-A_f)\,\mu_0(\Delta H)] \quad (3)$$

where N is the number of the turns of the sensing coil, A_0 and A_f stand for cross areas of the sensing coil and the steel rod respectively. The first part of the right side of Equation 3 corresponds to the flux variation along the steel rod, while the second part indicates the

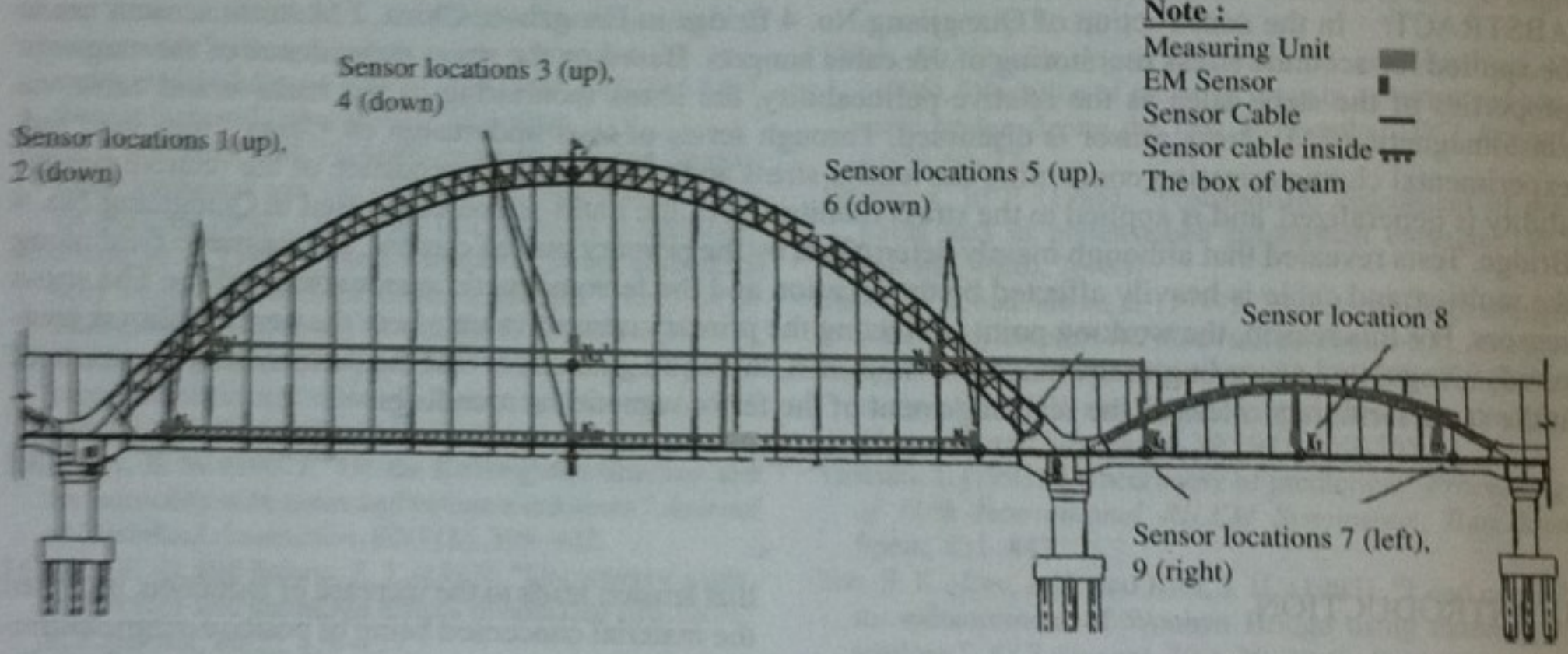

Figure 1. Indicative plot for EM sensor stress monitoring locations.

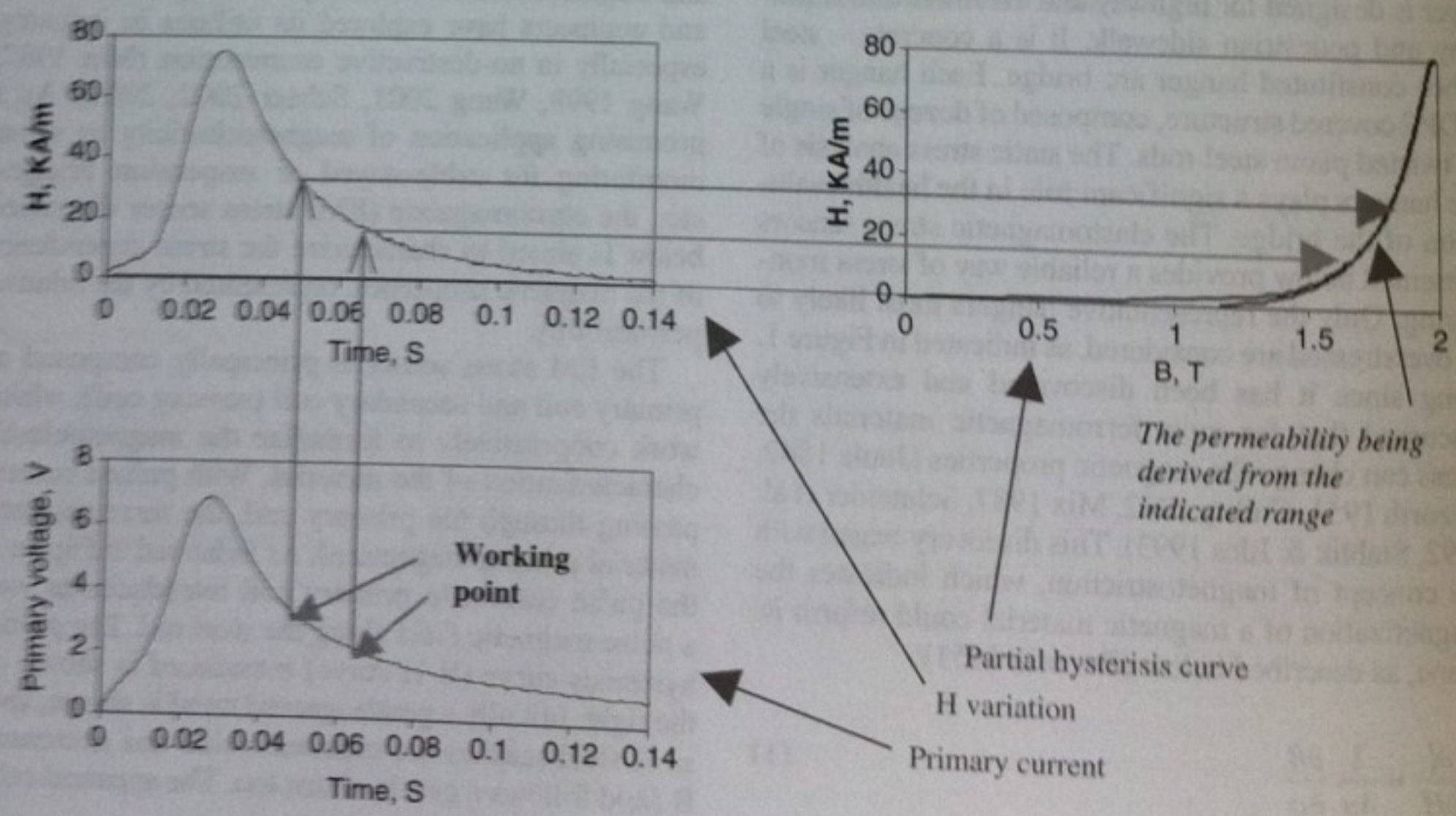

Figure 2. Primary current, magnetic field and hysterisis curve correlation of 7 mm piano steel rod, primary current = primary voltage/0.6Ω.

flux variation through the space gap between the steel rod and the secondary coil.

If without the rod in the secondary coil, but with the same pulsed current provided, within another time interval $\Delta t2$ during which the induced ΔH remains the same as in Equation 3, there is

$$\Delta\Phi_2=N[A_0\mu_0(\Delta H)] \quad (4)$$

Divided (3) by (4), and with $\mu = \mu_0\Delta B/\Delta H$, we have

$$\mu(\sigma,T)=\frac{A_0}{A_f}\left(\frac{\Delta\Phi_1}{\Delta\Phi_2}-1\right) \quad (5)$$

According to Farady's Law, there is $V = -\Delta\Phi/\Delta t$, So $\Delta\Phi_1 = \int_{\Delta t1} V dt$, and $\Delta\Phi_2 = \int_{\Delta t2} V dt$.

The time boundaries of the integration are determined by the working points – certain current values along the primary pulsed current (usually in the descending section), which determine the H field within the primary coil (Griffths 1999). It should be noted that the relative magnetic field should be high enough to technically saturate the steel rod.

Therefore the relative permeability of the steel rod could be rewritten into

$$\mu(\sigma,T) = 1+\frac{A_0}{A_f}\left[\frac{V_{out}(\sigma,T)}{V_0}-1\right] \quad (6)$$

where μ means permeability, σ is tensile stress, T is temperature, V_{out} indicates the integrated voltage with the rod in the solenoid while V_0 is the integrated voltage without the rod in the solenoid.

Through calibration, the temperature and stress dependence of the relative permeability is revealed. Such characterization is therefore used in stress monitoring of the steel rod. With temperature and relative permeability measured, the tensile stress could be calculated.

2 EXPERIMENTS

Primary and secondary coils are carefully wound on the plastic bobbin with a diameter slightly larger than that of the steel rod. The auxiliary parts, such as the precise temperature sensor and the hall sensors are mounted stably on the bobbin. The coils are sealed in the steel tube, with polyurethane resin filled up the seam to stabilize and protect the components. The EM stress sensor manufactured in the Infrastructures Sensor Technology Laboratory of the University of Illinois. At Chicago (UIC) is shown in Figure 3, and the indicative sketch is given in Figure 4.

The Power Stress Measurement System (PSM System), composed of the hardware and software, is innovated in the Infrastructures Sensor Technology Laboratory UIC. The PSM System can principally undertake the following tasks. (I) It provides a large pulsed current to magnetize the steel rod or cable. (II) It picks up the signals from the primary coil, secondary coil, hall sensors as well as temperature sensor and demonstrates them visually on the computer screen. (III) Together with the updated design of EM sensor, it guarantees the magnetic field correspondence of the permeability measured. (IV) Through delicately compiled software, it automatically integrates the current from the secondary coil and computes the relative permeability. (V) Through multiplexers and logic switches, each system unit can sequentially manipulate dozens of EM stress sensors. With all the above capabilities condensed into a portable volume, The PSM System is easy to handle, maintain and duplicate, which signifies its practical and magnificent prospect in Civil, Mechanical, as well as Materials Engineering.

Tests were first run on the 7 mm rod, as a result the magnetoelastic characterization with the influence factor of temperature is obtained. Then its utilities on the stress monitoring of multi-strand cable were discussed. The undesired effect of the EM sensor location uncertainties is excluded by proper calibration strategy. The PSM working chart are shown in Figure 5.

3 RESULTS AND ANALYSIS

3.1 *Tests on China 7 mm rod*

In order to reveal the tensile stress and temperature dependence of the relative permeability of the material, tests were run on China 7 mm rod with the Power Stress Measurement (PSM) System. The pulse current provided by the equipment must be high enough to technically saturate the rod for the consideration of accuracy and repeatability. Through calibration, a stable magnetoelasticity function of the steel rod should be

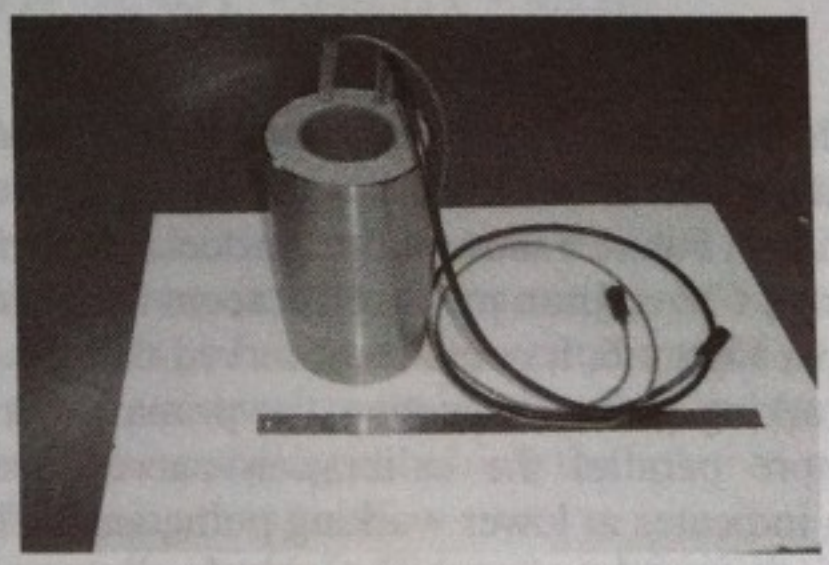

Figure 3. Picture of the EM sensor for Φ97 mm cable used in Qianjiang No. 4 bridge.

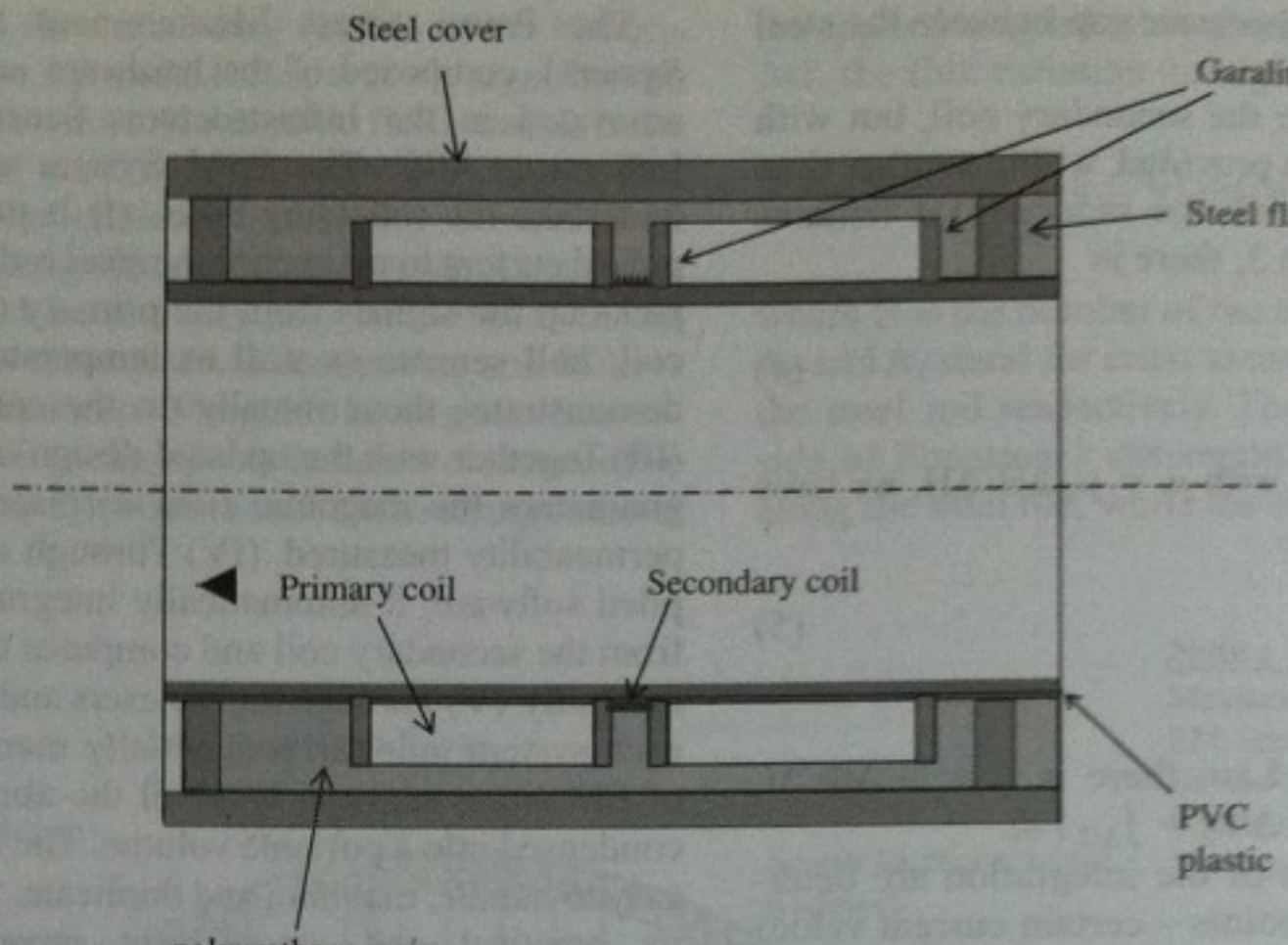

Figure 4. Indicative sketch of EM stress sensor.

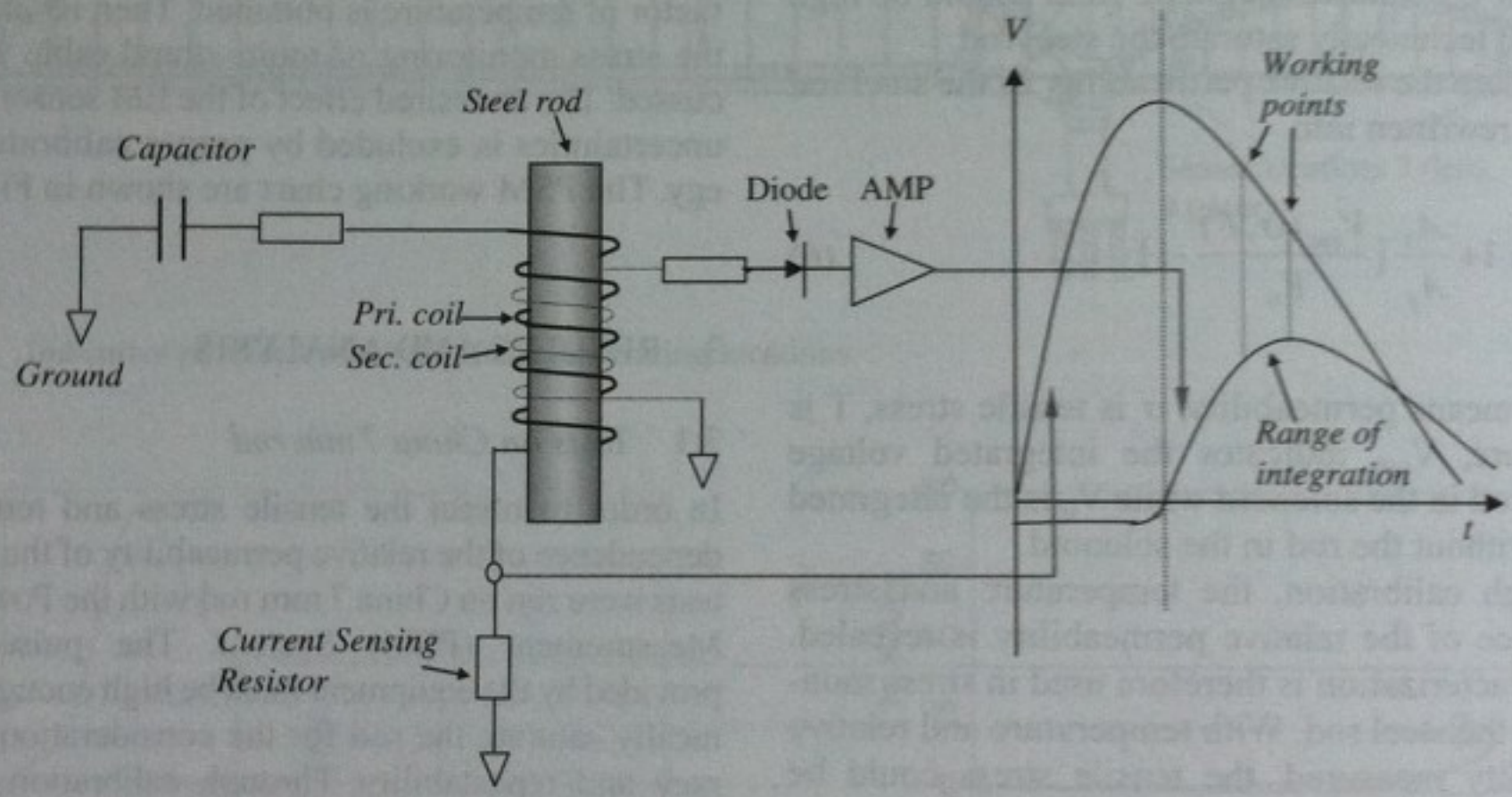

Figure 5. Working chart Pulse Magnetic Measurement System developed in the Infrastructures Sensor Technology Laboratory of UIC.

revealed, together with the influence factor of the temperature. Here the relative permeability is derived via Equation 5. Figure 6 shows the magnetoelastic characterization of China 7 mm piano rod at room temperature.

From Figure 6, it could be observed that the lower the working point (indicating the primary current), the more parallel the calibration curves become, which indicates at lower working point, small fluctuation in original permeability only leads to parallel shift of the calibration curve. However, with too low the working point, the relative permeability is calculated at the magnetic field far below technical saturation, which causes large error and low repeatability. By thorough comparison, the calibration expression tested under the working point of 0.73–0.53 V at 26.4°C is selected from Figure 6:

$$\sigma = 4.6804(\mu(\sigma, T=26.4°C))^2 + 214.34(\mu(\sigma, T=26.4°C)) - 1259.1 \quad (7)$$

where σ is stress in Mpa, and $\mu(\sigma, T = 26.4°C)$ means the relative permeability at stress σ and temperature

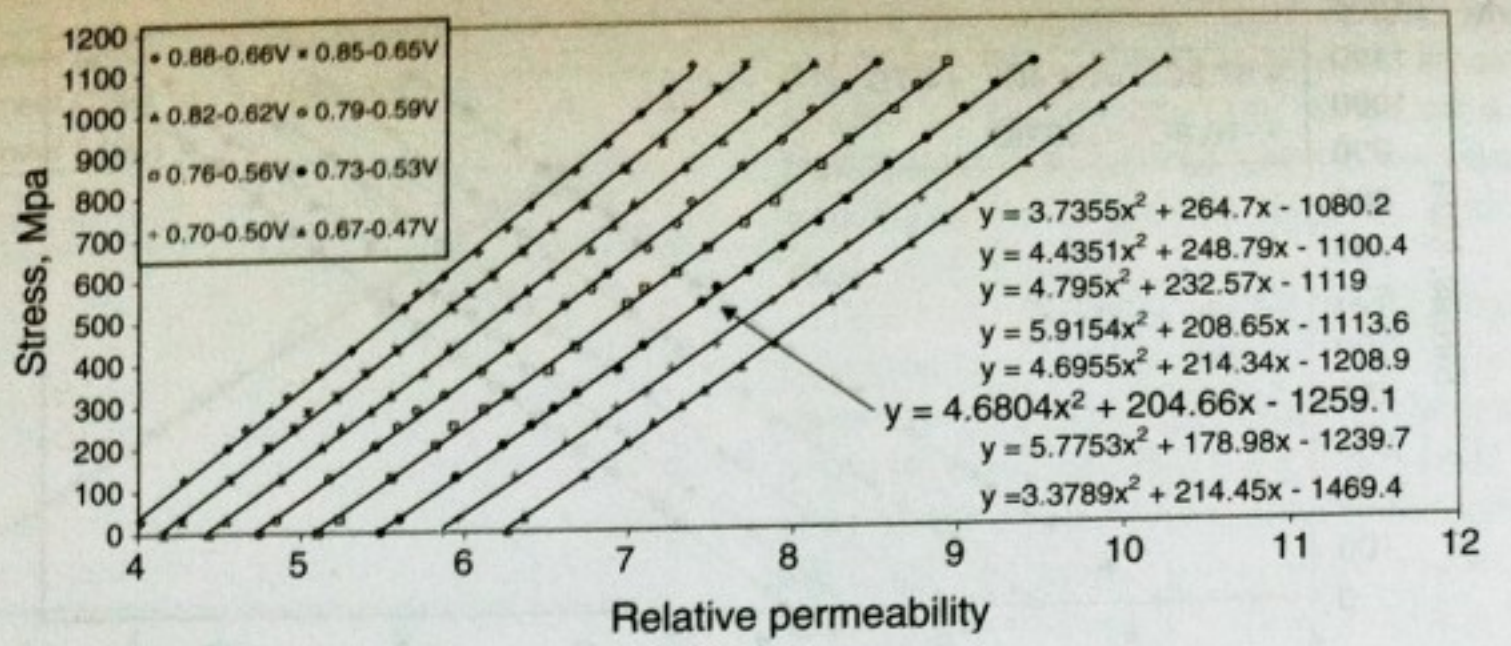

Figure 6. Stress versus permeability value at 26.4°C.

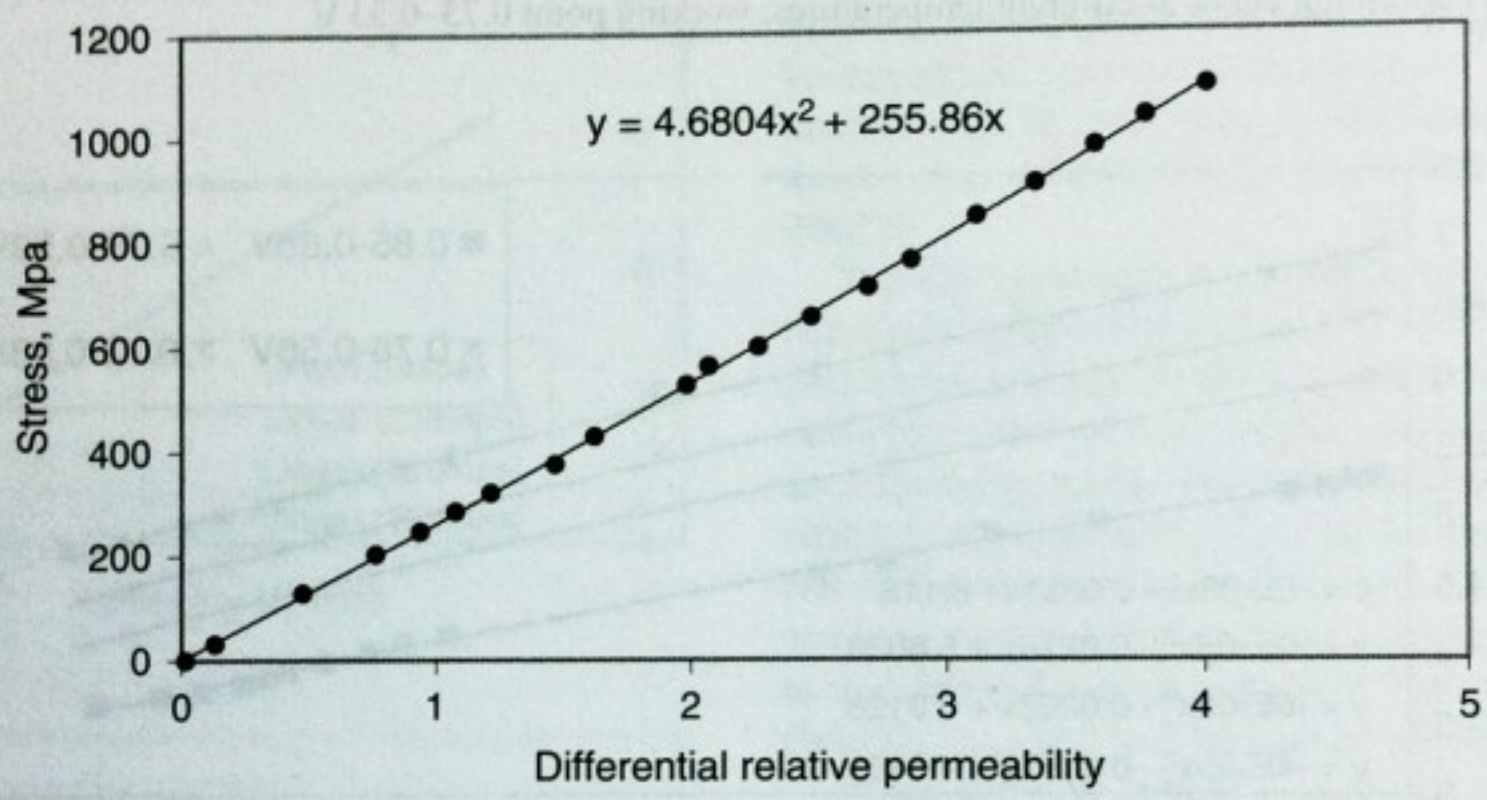

Figure 7. Stress vs. differential permeability when temperature is 26.4°C, working point is 0.73–0.53 V.

of 26.4°C. Equation (7) can be modified into the following form:

$$\sigma = 4.6804(\mu(\sigma, 26.4°C)-\mu(0, 26.4°C))^2 + 255.86(\mu(\sigma, 26.4°C)-\mu(0, 26.4°C)) \quad (8)$$

where $\mu(0, 26.4°C)$ is the relative permeability of the stress free steel rod measured at 26.4°C, which is 5.47. Here $(\mu(\sigma, 26.4°C)-\mu(0, 26.4°C))$ is defined as differential relative permeability at temperature 26.4°C, its correlation with stress is shown in Figure 7.

However, with temperature fluctuation, the calibration curve shifts obviously in a parallel manor, as illustrated in Figure 8. This experimental observation is consistent with previous research in UIC (Chen 2000).

Therefore, with the role of the temperature in permeability measurement of the stress free steel rod revealed, the relative temperature–permeability correlation at any stress could be inferred. Tests were run in order to find out how the permeability of stress free rod is affected by temperature, with outcome demonstrated in Figure 9. In natural environment, the differential thermal error should be taken into the consideration. Therefore the temperature measured at severe thermal fluctuation should be avoided (Lloyd et al. 2002).

Given the working point of 0.73–0.53 V, the function of permeability vs. temperature for the stress-free steel rod can be expressed as

$$\mu(0, T)= -5E\text{-}05T^2 - 0.0231T + 6.118, \quad (9)$$

which is given in Figure 9. $\mu(0, T)$ means the relative permeability of stress free steel rod at temperature T, T is the value of the temperature with the unit of °C. Another key step in stress monitoring is to express the tensile stress as a function of temperature and $\mu(\sigma, T)$, with fixed working point (indicating the primary current corresponding to which the relative permeability is being measured).

The results shown in Figure 8 and from the previous research in UIC indicate that the differential relative permeability $(\mu(\sigma, T)–\mu(0, T))$ is experimentally

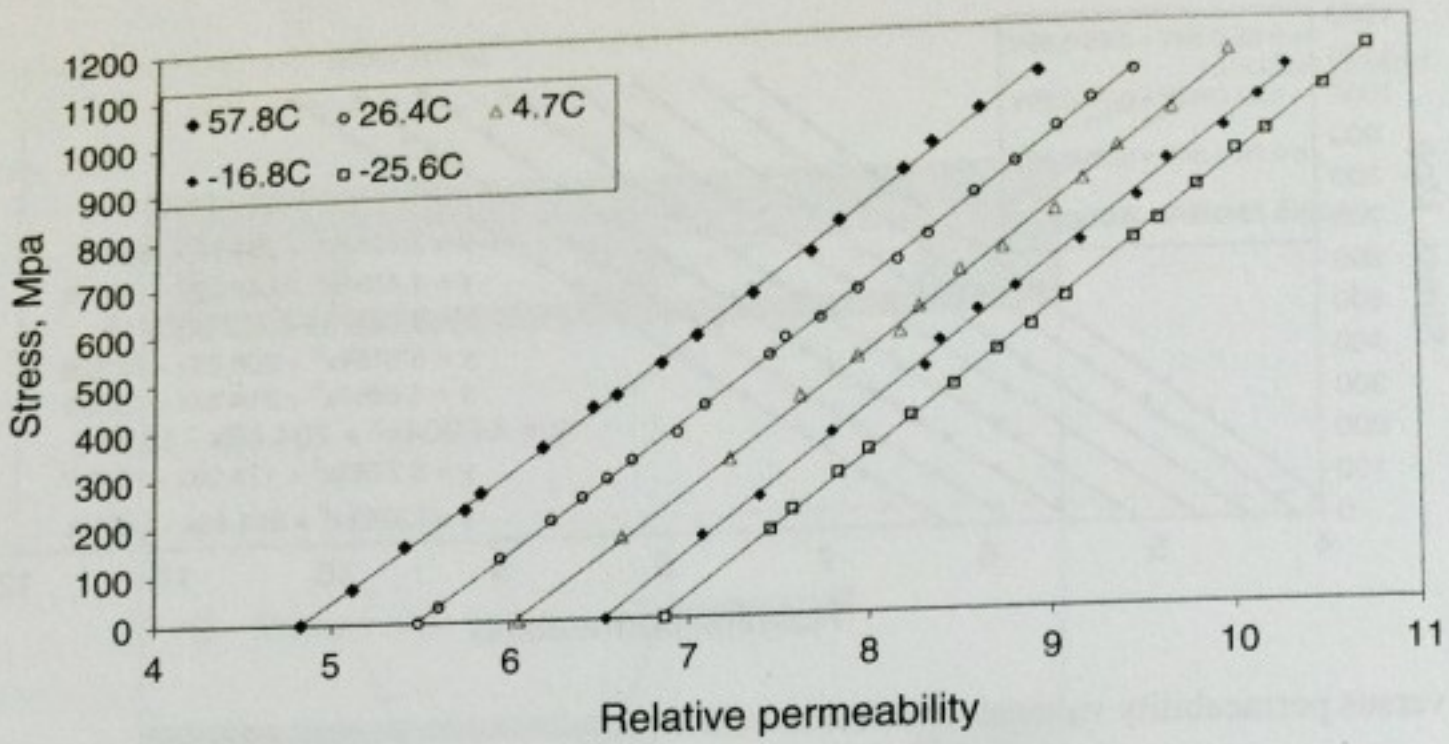

Figure 8. Stress calibration curve at different temperatures, working point 0.73–0.53 V.

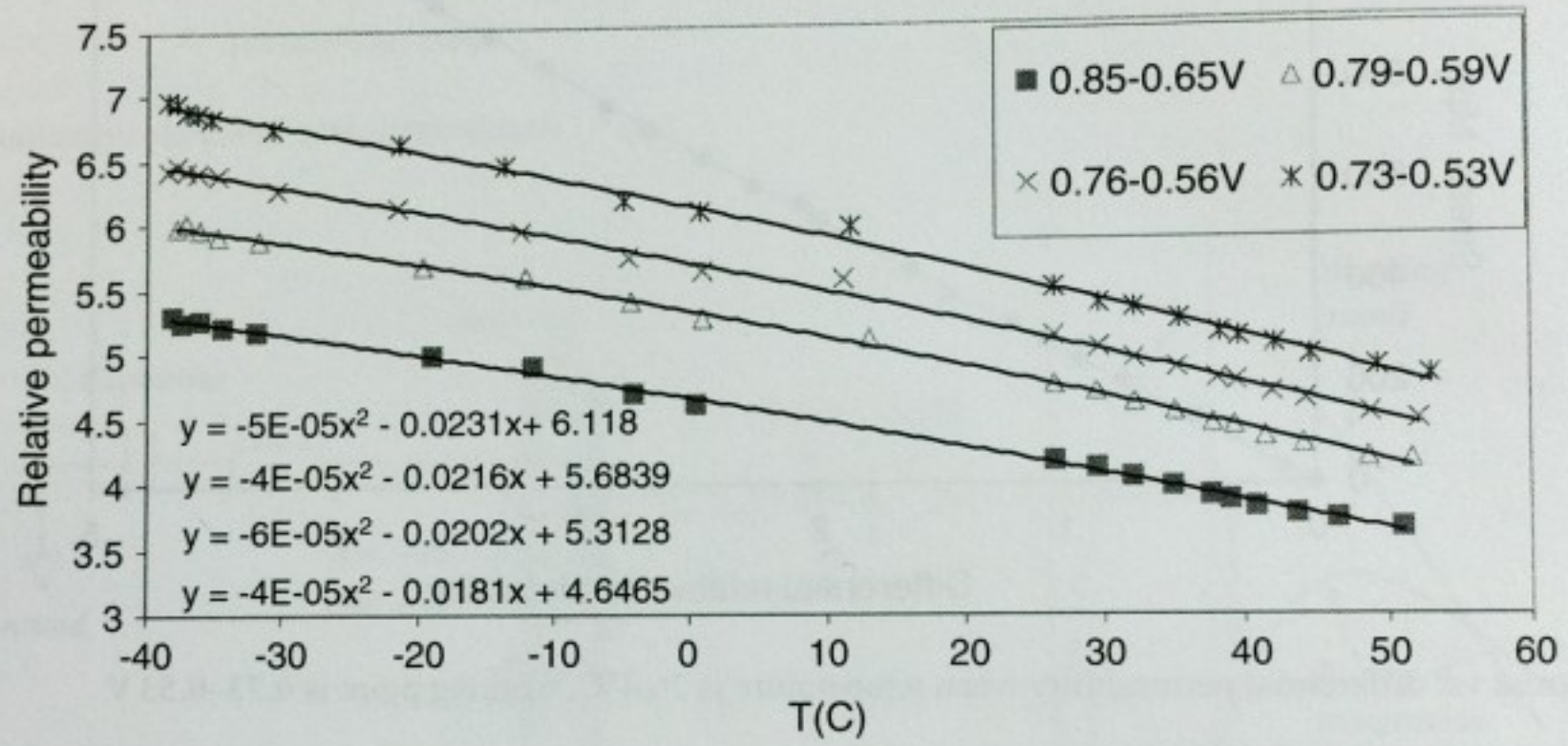

Figure 9. Temperature dependence of the relative permeability for stress free China 7 mm rod.

constant, provided the working point fixed. Therefore we have the stress calibration expression rewritten from Equation 7:

$$\sigma = 4.6804(\mu(\sigma, T)-\mu(0, T))^2 + 255.86(\mu(\sigma, T)-\mu(0, T)) \quad (10)$$

and

$$\mu(0, T)= -5E\text{-}05T^2 - 0.0231T + 6.118, \quad (9)$$

Through the above calibration functions, and given T and permeability $\mu(\sigma, T)$, the tensile stress can be calculated. It should be noted that the relative permeability $\mu(0, T)$ must be measured at the proper working point as long as Equation 8 holds. That working point remains unchanged during the EM magnetoelastic calibration of the China 7 mm steel rod, provided the EM sensor not relocated. In the following paragraphs, the application of Equation 8–9 in stress monitoring of multi-strand cable will be described. As given in the introduction part, the relative permeability is calculated from the integration of the sensing voltage, with the time boundaries defined by the working point (primary voltage value, in lieu of primary current). Does the fixed working point the relative permeability derived from always corresponds the same magnetic field along the steel rod? Figure 10(a) and 10(b) indicates that the correlation of magnetic field and primary current is not sensitive to temperature and stress variation. However, the EM sensor location plays a significant role, as shown in Figure 10(c), because relocation of the EM sensor rearranges the ferromagnetic surroundings, thus changes the magnetic field distribution. Therefore in calibration, the ferromagnetic surroundings should be kept undisturbed. However, the drawback of location effect is to

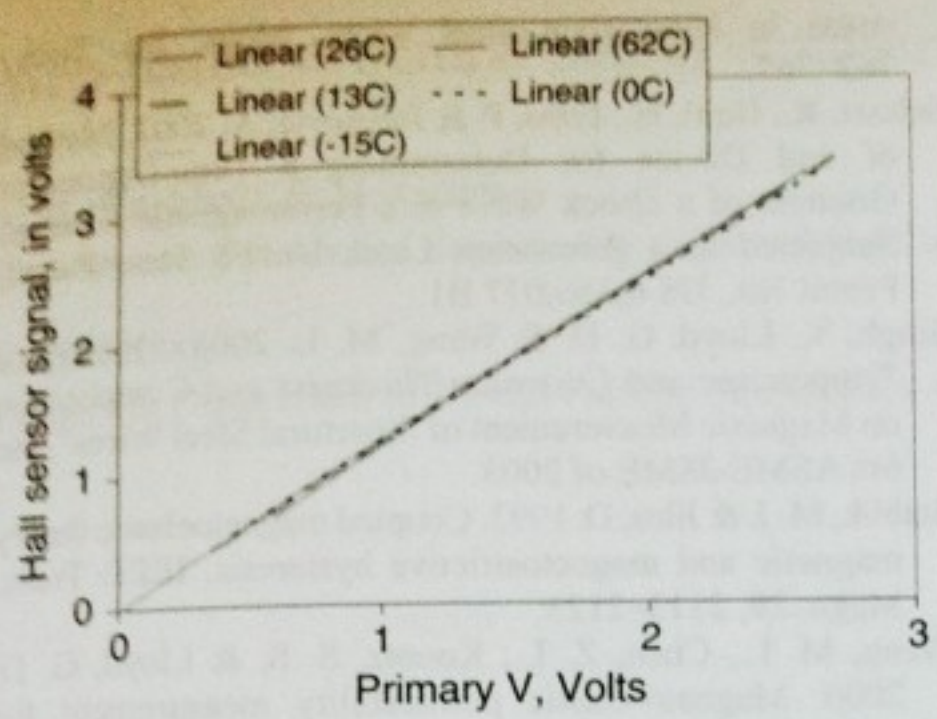

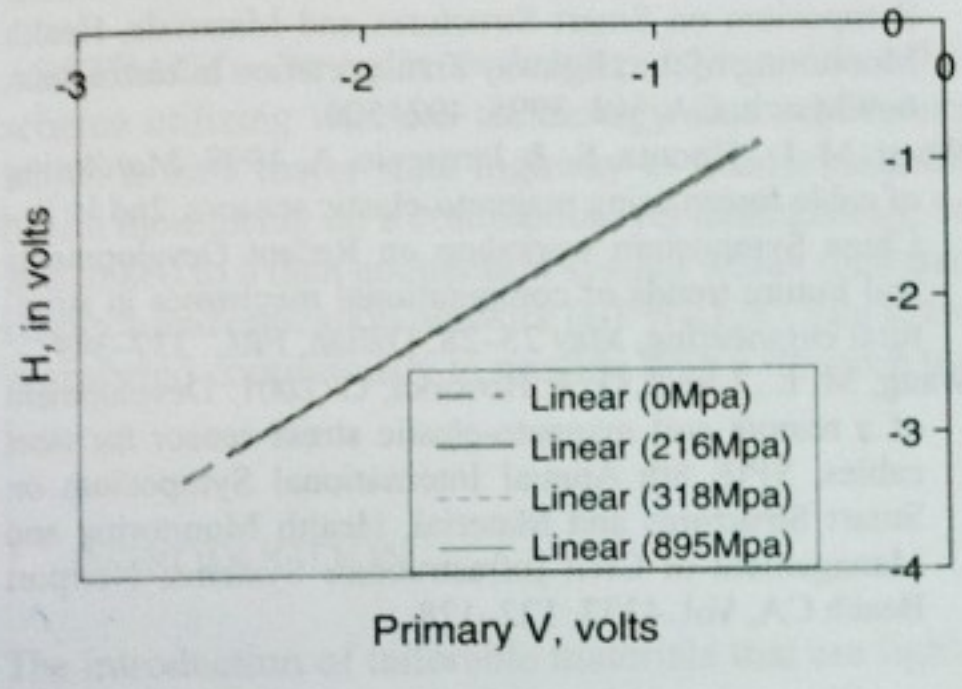

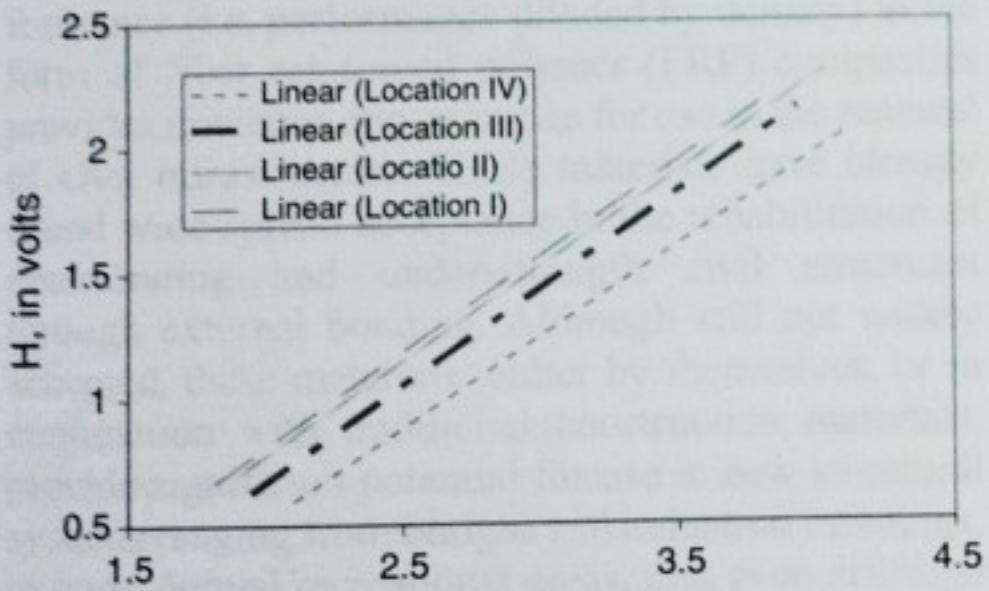

Figure 10. Magnetic field vs. primary current (= primary V/0.6Ω) at (a) different temperature of 7 mm rod, (b) different stress of 7 mm rod, and (c) different location of the EM sensor along the 37_7 mm multi-strand cable.

be excluded by proper EM sensor calibration, as discussed below.

3.2 *Calibration procedures on multi-strand cable*

For the multi-strand cable consisting of dozens of single steel rods, the elastomagnetic properties are similar to that of the single rod. Tests in UIC showed that the measured stress of each single rod by average is equal to that of the multi-strand cable as a whole (Chen 2000). Therefore the calibration functions – Equation 9 and Equation 8 can be used in multi-strand cable stress monitoring.

Due to its dramatic effect on the magnetic field distribution, the uncertainty of the EM sensor location does not guarantee the fixed correspondence of the working point and the magnetic field. Therefore it is very likely that the calibrated permeability $\mu(0, T)$ and the in-situ measured permeability $\mu(\sigma, T)$ are derived from different magnetic field, thus not comparable.

In this project, the EM sensor design was modified, aimed to solve the above problem that puzzled the engineers devoted to precise stress sensing. In the updated design of the EM sensor, magnetic field is to be inspected, and the working point was determined accordingly. The magnetic field distribution in the EM sensor was systematically studied in UIC (Hovorka 2002).

The key point in this calibration strategy is to ascertain the magnetic field where the relative permeability should be measured. With a stress free multi-strand cable provided, we first roughly find the working point corresponding to the magnetic field around 25 KA/m, which is an experimental value for the specific material concerned in this project, then finely regulate the working point till the measured permeability is equal to that derived from Equation 4. The relative magnetic field $H_{standard}$ is fixed during the stress monitoring.

When the EM sensor is mounted onto the erected cable, the working point should be recalibrated in accordance with $H_{standard}$. Then with the measured permeability, the tensile stress could be calculated through Equation 5. If the ferromagnetic surroundings of the EM sensor are rearranged, the working point must be calibrated again. Otherwise with the magnetic field distribution undisturbed, the working point remains constant.

4 CONCLUSIONS

The calibration method for the stress monitoring of the multi-strand cable was discussed in this paper. The magnetoelastic characterization of the steel with the effect of the temperature was obtained through tests conducted on the 7 mm single steel rod. In order to apply the calibration functions to the stress monitoring of the multi-strand cable, a technically satisfied correspondence of permeability and magnetic field must be guaranteed. Several influencing factors of the magnetic field were studied. Tests showed that the magnetic field is hardly dependent on temperature and stress, in respect to the engineering application of the EM stress sensor. However it can be obviously shifted

with the EM stress sensor relocated along the steel cable. The working point must be regulated according to the magnetic field.

REFERENCES

Bozorth, R. M. 1951. Ferromagnetism, D. Van Nostrand Company, INC., Canada.

Chen, Z. 2000. Characterization and Constitutive Modeling of Ferromagnetic Materials for Measurement of Stress, PhD thesis, the Univ. of Ill. at Chicago.

Cullity, B. D. 1972. Introduction to Magnetic Materials, Addision-Welsley Publishing Company, Reading MA.

Griffths, D. J. 1999. Introduction to Electrodynamics, 3rd Edition, Prentice Hall, Inc.

Hovorka, O. 2002. Measurement of Hysterisis Curves for Computational Simulation of Magnetoelastic Stress Sensors, MS thesis, the Univ. of Ill. at Chicago.

Lloyd, G. M., Singh, V. & Wang, M. L. 2002. Experimental evaluation of differential thermal errors in magnetostatic stress sensors for Re <180, IEEE Sensors 2002, Magnetic Sensing III, Paper No. 6.54.

Mix, P. E. 1987. Introduction to nondestructive testing, John Wiley & Sons, Inc., Hoboken, NJ.

Joule, J. P. 1842. On a new class of magnetic forces, Ann. Electr. Magn. Chem. 8, 219–224.

Kvasnica, B. & Fabo, P. 1996. Highly precise non-contact instrumentation for magnetic measurement of mechanical stress in low-carbon steel wires, Meas. Sci. Tech., 763–767.

Schaer, R., Boni, H., Fabo, P. & Jarosevic, A. 2002. Method of and Device for Determining a Time-Dependent Gradient of a Shock Wave in a Ferromagnetic Element Subjected to a Percussion Load, United State Patent, Patent No., US 6,356,077 B1.

Singh, V., Lloyd, G. D. & Wang, M. L. 2003. "Effects of Temperature and Corrosion Thickness and Composition on Magnetic Measurement of Structural Steel Wires", the 6th ASME-JSME of 2003.

Stablik, M. J. & Jiles, D. 1993. Coupled magnetoelastic theory magnetic and magnetostrictive hysteresis, IEEE Trans. Magn. 29, 2113–2123.

Wang, M. L., Chen, Z. L., Koontz, S. S. & Lloyd, G. D. 2000. Magneto-elastic permeability measurement for stress monitoring, In Proceeding of the SPIE 7th Annual Symposium on Smart Structures and Materials, Health Monitoring of the Highway Transportation Infrastructure, 6–9 March, CA, Vol. 3995, 492–500.

Wang, M. L., Koontz, S. & Jarosevic, A. 1998. Monitoring of cable forces using magneto-elastic sensors, 2nd U. S. - China Symposium workshop on Recent Developments and Future trends of computational mechanics in structural engineering, May 25–28, Dalian, PRC. 337–349.

Wang, M. L., Lloyd, G. & Hovorka, O. 2001. Development of a remote coil magneto-elastic stress sensor for steel cables, SPIE 8th Annual International Symposium on Smart Structures and Material, Health Monitoring and Management of Civil Infrastructure Systems; Newport Beach CA, Vol. 4337, 122–128.